Optical spectra and local structure of Eu^{3+} ions doped in Nb_2O_5-La_2O_3-B_2O_3-BaO glasses

Haiping Xia (夏海平), Jianli Zhang (章践立), Jinhao Wang (王金浩), and Yuepin Zhang (张约品)

Laboratory of Photo-Electronic Materials, Ningbo University, Ningbo 315211

Received November 25, 2005

The $x$$Nb_2O_5$-(15−$x$)$La_2O_3-40B_2O_3$-45BaO ($x$ = 5, 7.5, 12.5 mol%) glasses doped with Eu^{3+} ions in 1 mol% are fabricated by the melting method. The Fourier transform infrared (FTIR) spectra, phonon sideband spectra, emission and excitation spectra of the glasses are measured. The crystal field parameter and coordination number of Eu^{3+} ions in the glasses are obtained according to the splitting of their $^5D_0 - {}^7F_1$ levels. The intensity parameters Ω_2 and Ω_4 of Eu^{3+} ions for optical transition are calculated from their emission spectra in terms of reduced matrix $U^{(t)}$ (λ = 2, 4, 6) character for optical transitions. The results indicate that the intensity parameters Ω_2 and Ω_4 increase with the increase of Nb_2O_5 content, suggesting that the symmetry becomes lower, the band of Eu and O atoms becomes stronger and the covalence increases with the increase of Nb_2O_5 content.

OCIS codes: 160.5690, 160.2750, 160.2540, 070.4790.

Oxide glasses are favorable as the host materials for functional ions and molecules due to their chemical/physical stability, easy mass production, high transparency, and compositional variety. Glasses containing Eu^{3+} ions have attracted much attention because of their various applications in optical devices such as lasers, phosphors, and optical data storage[1,2]. Because the structure and environment of the glass strongly influence the fluorescence characteristics of Eu^{3+} ions such as the splitting of Stark energy level, actually, Eu^{3+} ions are also an activator to study local structure and crystal field effect. Knowledge of local structure surrounding rare earth ions in glasses is important not only for explaining their optical properties but also for designing novel laser glasses[3−7].

It has been found that the stimulated emission cross section (σ_e) of Yb^{3+} ion can be enhanced by replacing Nb_2O_5 with suitable amount of P_2O_5, SiO_2, and B_2O_3 in phosphate and borate glasses[8], and La_2O_3[9] with modifiers in borate glass. Because the rare earth elements have similar chemical properties and diameters, the Eu^{3+} ions in the above glass show similar enhanced σ_e to that of Yb^{3+} ions. Nb_2O_5 and La_2O_3 are important chemical agents of glasses. However, they are seldom used together as glasses compositions. In this work, we prepared the Eu^{3+}-doped Nb_2O_5-La_2O_3-B_2O_3-BaO glasses and investigated their optical properties.

The Judd-Ofelt (J-O) theory[10,11] is the most useful theory in estimating the forced electric dipole transitions of rare earth ions in various environments. In the J-O theory, three parameters Ω_2, Ω_4, and Ω_6 appear and can be determined experimentally from the measurements of absorption spectra and some chemical/physical properties of host. From these parameters, several important optical properties, e.g., the oscillator strength, the radiative transition probability, and the spontaneous emission probability, can be evaluated. This method has been adopted and used widely. However, it is not available for opacity and the matrices with strong absorption, in which their optical absorptions are difficult to be obtained. Recently, the intensity parameters Ω_2 and Ω_4 of Eu^{3+} for optical transition were calculated from their emission spectra in terms of reduced matrix $U^{(t)}$ (λ = 2, 4, 6) character for optical transitions[12], which made good implement to the J-O theory. The similar method is also adopted in this paper to calculate the intensity parameters. The relationship between the fluorescent properties and the local structure surrounding Eu^{3+} ions is also primarily investigated according to the splitting of $^5D_0 - {}^7F_1$ energy levels.

Three kinds of compositions of glasses doped with Eu^{3+} ions are used in this study, they are: S1, 5Nb_2O_5-10La_2O_3-45BaO-40B_2O_3; S2, 7.5Nb_2O_5-7.5La_2O_3-45BaO-40B_2O_3; S3, 12.5Nb_2O_5-2.5La_2O_3-45BaO-40B_2O_3. BaO and B_2O_3 were introduced in the forms of $BaCO_3$ and $B(OH)_3$. La_2O_3, Nb_2O_5, and Eu_2O_3 were introduced directly from their oxide compounds. All the chemicals are 99.9% purity. The batches of 50 g were mixed in an Al_2O_3 crucible under air atmosphere. After keeping at 1200 °C for 2 h, the melted glass was poured on to a stainless steel plate. Each glass was annealed at 300 °C for 3 h and then cooled to room temperature. The sample was cut into small pieces and well polished.

The infrared (IR) spectra of samples were recorded with a Shimadzu FTIR-4800s Fourier transform infrared (FTIR) spectrometer. The samples were prepared using the KBr pellet technique. The excitation and spectra were recorded with a Hitachi F-4500 fluorescence spectrometer by monitoring the $^5D_0 - {}^7F_2$ emission at 614 nm. By excitation spectra, the phonon sideband associated with the $^7F_0 - {}^5D_2$ zero phonon transition was obtained in the range of 430—465 nm. The emission spectra were obtained under the excitation of a 394-nm light.

Figure 1 shows the excitation spectra of the Eu^{3+}-doped glasses. Sharp lines were observed at 364, 384, 396, 416, 466, 534, 579 nm, respectively. These lines are associated with the f-f transitions of Eu^{3+} ions. Their detailed origins are labeled in the figure. It can be seen from Fig. 1 that as the content of Nb_2O_5 in the glasses increases, the emission intensity decreases.

Figure 2 shows the emission spectra of Eu^{3+} ions in the

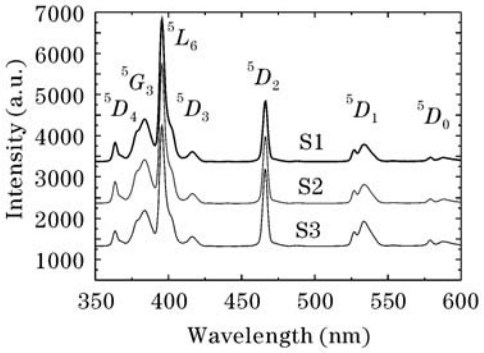

Fig. 1. Excitation spectra of different samples.

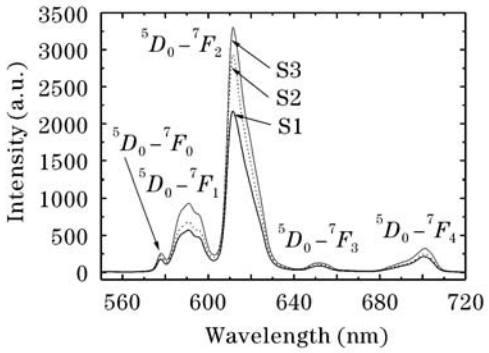

Fig. 2. Emission spectra of different samples.

above glasses. The emission peaks of $^5D_0-{}^7F_J$ ($J=0$, 1, 2, 3, 4) transitions at 578, 591, 612, 652, and 702 nm can be observed, indicating that Eu^{3+} ions are incorporated. It can be noticed from Fig. 2 that the emission intensity increases with the decrease of Nb_2O_5 content. The emission intensity of $^5D_0-{}^7F_2$ transition at 612 nm is the strongest. The transition of $^5D_0-{}^7F_6$ level at $\sim$ 800 nm was difficult to be observed in experiments[12] due to its small transition rate. So the parameter Ω_6 is not obtained in this paper. The refractive index is calculated according to the method of Ref. [13], which was used widely to estimate the refractive index of glasses and the obtained refractive index can be near to the real one exactly.

In the emission spectra, the $^5D_0-{}^7F_J$ ($J=2$, 4, 6) transition is electric-dipole-allowed and its intensity is sensitive to the local structure around Eu^{3+}. On the other hand, the $^5D_0-{}^7F_J$ ($J=1$, 3, 5) transition is magnetic-dipole-allowed and its intensity shows little variation with the crystal field strength on Eu^{3+}. In general, the intensity ratio of the electric-dipole to magnetic-dipole transition is widely used for the study of chemical bond between anions and the rare earth ions.

The electric dipole transition rate of $^5D_0-{}^7F_J$ ($J=2$, 4, 6) can be written as[12]

$$A_{\rm ed}=\frac{64\pi^4e^2}{3h}\frac{\overline{\nu}^3}{2J'+1}\frac{n(n^2+2)^2}{9}\times\sum_{t=2,4,6}\Omega_t\langle\varphi J\|U^t\|\varphi' J'\rangle^2, \quad (1)$$

where e and n are the electron mass and glass refractive index, respectively; $\overline{\nu}$ is the central wavenumber of the transitions; h is the Plank constant; J' is the total number of angular momentum of the initial energy level; $\langle\varphi J\|U^t\|\varphi' J'\rangle$ is the reduced matrix element from state of $|\varphi' J'\rangle$ to $\langle\varphi J|$, which are approximately unchanged for different matrices[12].

The magnetic dipole transition rate $^5D_0-{}^7F_1$ is given by

$$A_{\rm md}=\frac{64\pi^4}{3h}\frac{\overline{\nu}^3}{2J'+1}n^3S_{\rm md}, \quad (2)$$

where $S_{\rm md}$ is the magnetic dipole operator and a constant of 1.07×10^{-41} can be calculated from hybrid wavefunction[7,14], Ω_t is the intensity parameter.

The intensity ratio of the electric dipole to magnetic dipole transition is deduced as

$$\frac{\int I_J(\sigma)\mathrm{d}\sigma}{\int I_{\rm md}(\sigma)\mathrm{d}\sigma}=\frac{e^2\sigma_J^3(n^2+2)^2}{9n^2S_{\rm md}\sigma_{\rm md}^3}\Omega_t\times\langle\psi J\|U^t\|\psi' J'\rangle^2. \quad (3)$$

Based on Eq. (3) and the fluorescence intensity ratios of $^5D_0-{}^7F_2/{}^5D_0-{}^7F_1$ and $^5D_0-{}^7F_4/{}^5D_0-{}^7F_1$, omitted the "J hybridization" caused by crystal field, the values of Ω_2 and Ω_4 could be obtained, as shown in Table 1. The variation of Ω_2 and Ω_4 with contents of La_2O_3 and Nb_2O_5 in glasses is shown in Fig. 3.

Because the emission spectra could be obtained in almost all of luminous materials, and the method of calculating the parameters from their emission spectra was simple, and moreover, the error was smaller in comparison with that from their absorption spectra, the method was favorable and effective. Actually, Ω_2 presents the ligand symmetry and the structure order. The larger the value of Ω_2 is, the stronger the covalency and the lower the symmetry of glass are. It can be seen from Fig. 3 that the values of Ω_2 in the glasses increase with the content of Nb_2O_5, indicating that the covalency of glass

Table 1. Intensity Ratios of $^5D_0-{}^7F_2/{}^5D_0-{}^7F_1$ (I_2/I_1) and $^5D_0-{}^7F_4/{}^5D_0-{}^7F_1$ (I_4/I_1), and the Intensity Parameters Ω_2, Ω_4 for Different Samples

	$n_{\rm D}$	I_2/I_1	I_4/I_1	Ω_2 ($\times10^{-20}$ cm^2)	Ω_4 ($\times10^{-20}$ cm^2)
S1	1.8395	1.69	0.314	5.18	1.21
S2	1.8470	1.62	0.321	5.34	1.13
S3	1.8620	1.50	0.298	6.17	1.16

$n_{\rm D}$: the refractive index at 589.3 nm (the D Fraunhofer line).

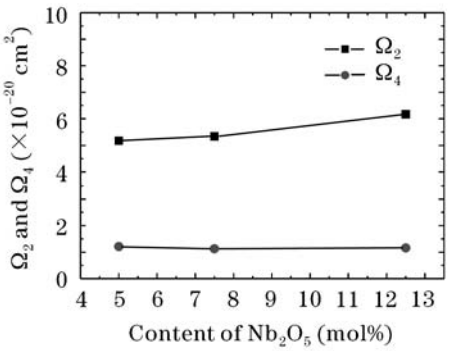

Fig. 3. Variation of Ω_2 and Ω_4 with content of Nb_2O_5.

becomes stronger and the symmetry becomes lower, Nb_2O_5 shows more impact to improve the covalency of glass compared with La_2O_3. B_2O_3 and Nb_2O_5 are the formation of glass network, and La_2O_3 and BaO are the modifiers of glass network. However, the introduction of the modifiers into glass takes great effects on the optical properties and structure of glass[8,9].

Phonon sideband of $^7F_0 - {}^5D_2$ excitation, taking from the spectra of $^5D_0$ emission, is a useful technique to investigate the local structure surrounding rare earth ion in the glass network[15,16]. Figure 4 shows phonon sideband spectra of Eu^{3+} ions in the niobate-lanthanum-borate glasses. Two bands of 420—860 cm^{-1} which was attributed to the $Nb-O$ bonds in the NbO_6 octahedra[17] and $\sim 870 - 1430$ cm^{-1} which was related to the B−O bonds in $[BO_3]$[18] were observed in Fig. 4. The phonon sidebands were corresponding to their Raman and IR vibration spectra. The FTIR spectra of the glasses were also recorded, as shown in Fig. 5. Three bands of 480—880, 880—1300, and 1300—1800 cm^{-1} can be observed in the figure (see the arrows).

It had been confirmed that, when Ba and La were introduced into borate glasses, the bonds of Ba(La)−O−B= are formed, which results in IR peak with smaller wavenumber compared with that of O−B=[19]. The former two bands in Fig. 5 were corresponding exactly to those shown in Fig. 4. The band of 880—1300 cm^{-1} should be assigned to the bonds of Ba(La)−O−B= and the one of 1300—1800 cm^{-1} to the bond of O−B=. It should be noted that the Ba−O vibrational modes in the range of 180—350 cm^{-1} do not appear in the phonon side spectra due to the concealment from the zero phonon lines of $^7F_0 - {}^5D_2$.

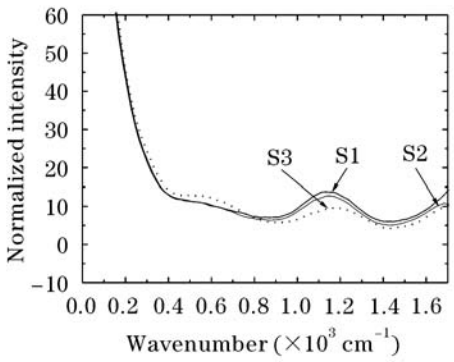

Fig. 4. Phonon sideband spectra of Eu^{3+} ions in different glasses. The excitation intensities of $^7F_0 - {}^5D_2$ are normalized in all the glasses.

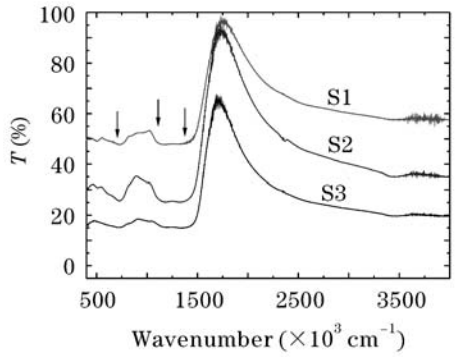

Fig. 5. FTIR spectra of different glasses. The arrows indicate three bands of 480—880, 880—1300, and 1300—1800 cm^{-1}.

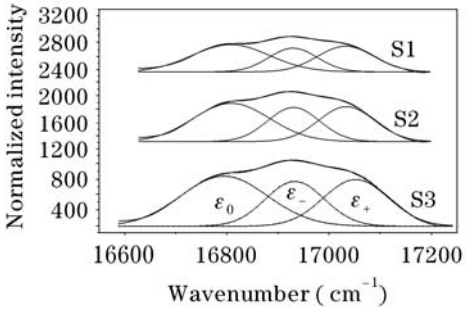

Fig. 6. Resolved emission spectra of the three crystal-field-splitting lines of the $^5D_0 - {}^7F_1$ transition at room temperature.

Figure 6 shows the fluorescence spectra of the $^5D_0 - {}^7F_1$ transition of Eu^{3+} in the glasses at room temperature. The fluorescence spectroscopy is useful and effective to study the local environment around the Eu^{3+} ions[3−8]. As shown, the lines could be completely resolved into three Gaussian components (ε_0, ε_-, ε_+), indicating that the Eu^{3+} ions were located in sites with a symmetry of C_{2v} or C_2 or Cs. The peak energies of the Stark components of $^7F_1$ are plotted in Fig. 6 as a function of chemical composition. It can be seen from Fig. 6 that the relative intensities of ε_0, ε_-, ε_+ in the glasses were almost same, they were 16793.81, 16936.70, and 17048.28 cm^{-1}, respectively.

In the above point symmetries, it was thought that the lowest energy of the $^7F_1$ lines could be assigned to the M_J=0 component of the $^7F_1$ level, which had a large electron distribution along the z-axis. On the other hand, the other two high energy components corresponded to the electron distribution along the x-y plane. Under these conditions, the z-axial and x-y plane components of the second-order crystal field parameters, B_{20} and B_{22}, could be estimated from the energies of the three $^7F_1$ lines as[6,7]

$$B_{20} = \frac{5}{3}[2E_{\varepsilon_0} - E_{(\varepsilon_+)} - E_{(\varepsilon_-)}], \tag{4}$$

$$B_{22} = \frac{5}{\sqrt{6}}[E_{(\varepsilon_+)} - E_{(\varepsilon_-)}]. \tag{5}$$

The calculated second-order crystal field parameters, B_{20} and B_{22}, were −662.3 and 227.8 cm^{-1}, respectively. Comparing the values with those in SiO_2, Al_2O_3-SiO_2, and P_2O_5-Nb_2O_5 glasses[7,19], the values in this glass were smaller than those in the silicate glass and bigger than those in the P_2O_5-Nb_2O_5 glasses, suggesting that the order of the host's effect on the Eu^{3+} ion is the silicate glasses, this glass, and P_2O_5-Nb_2O_5 glasses.

It is known that the value of B_{20} has a portion dependent on the bond distance, r, between the coordinating ligands and the center ion, which is given by

$$B_{20} \propto \frac{3Z^2 - r^2}{r^3}. \tag{6}$$

A smaller value of B_{20} implies longer distance between europium and oxygen. It can be seen from Fig. 6 that the B_{20} values are almost same in these glasses, indicating that the distance between europium and oxygen does

not change. Brecher and Riseberg *et al.*[3,4] analyzed these fluorescence line narrowing (FLN) spectra of the Eu^{3+} ions in oxide glasses and proposed geometric models for the coordination sphere of the Eu^{3+} ions. They restricted the ratio of the crystal parameters, B_{20}/B_{22}, to the coordination number of Eu^{3+} ions, in which the B_{22}/B_{20} values of -2.05 and -0.23 correspond to coordination values of 8 and 9, respectively. B_{20}/B_{22} was determined to be $-(2.91 \pm 0.30)$. This indicates that the coordination value of most Eu^{3+} ions is near 8, which is the same as the case of P_2O_5-Nb_2O_5 glasses[19]. However, the coordination value of Eu^{3+} in silicate glass is about 9[7]. From the above results, it can be known that the coordination of Eu^{3+} in various glasses is related to the glass structure and chemical composition of glass, although it was not known in detail yet.

In conclusion, the spectroscopic properties of the $x$$Nb_2O_5$-$(15-x)$$La_2O_3-40B_2O_3$-45BaO ($x$ = 5, 7.5, 10, 12.5 mol%) glasses doped with Eu^{3+} in 1 mol% were studied. The intensity parameter Ω_2 increases with the increase of Nb_2O_5 content. The band of Eu and O atoms becomes stronger and the covalence increases with the increase of Nb_2O_5 content. The introduction of Ba and La into glass results in forming a Ba(La)−O−B= bond with shorter wavenumber. The second-order crystal field parameters, B_{20} and B_{22}, were calculated to be -662.3 and 227.8 cm^{-1}, respectively, according to the splitting of energy levels, and the coordination value of most Eu^{3+} ions was estimated to be near 8. Such glasses containing Eu^{3+} with high stimulated emission cross section is expected to find applications in optical data storage and laser devices.

This work was supported by the Natural Science Foundation of Zhejiang Province (No. 502164) and the Doctoral Science Foundation of Ningbo (No. 2005A610010). H. Xia's e-mail address is hpxcm@nbu.edu.cn.

References

1. H. Xia, H. Song, Q. Nie, J. Zhang, J. Wang, J. Wang, T. Xu, and J. Zhang, Chin. Opt. Lett. **1,** 296 (2003).
2. Z. Zheng, H. Ming, X. Sun, and J. Xie, Chin. Opt. Lett. **3,** 605 (2005).
3. C. Brecher and L. A. Riseberg, Phys. Rev. B **13,** 81 (1976).
4. C. Brecher and L. A. Riseberg, Phys. Rev. B **21,** 2607 (1980).
5. M. Tanaka and T. Kushida, Phys. Rev. B **49,** 5192 (1994).
6. M. Tanaka, G. Nishimura, and T. Kushida, Phys. Rev. B **49,** 16917 (1994).
7. M. Nogami and Y. Abe, J. Appl. Phys. **81,** 6351 (1997).
8. X. Zou and H. Toratani, Phys. Rev. B **52,** 15889 (1995).
9. M. J. Weber, J. E. Lynch, D. H. Blackburn, and D. J. Cronin, IEEE J. Quantum Electron. **19,** 1600 (1983).
10. B. R. Judd, Phys. Rev. **127,** 750 (1962).
11. G. S. Ofelt, J. Chem. Phys. **37,** 511 (1962).
12. B. Chen, H. Wang, S. E, and S. Huang, Chin. J. Lumin. (in Chinese) **22,** 139 (2001).
13. F. Gan, *The Physical Property Calculation and Compositional Design of Inorganic Glasses* (in Chinese) (Shanghai Scientific and Technical Press, Shanghai, 1981) p.105.
14. V. G. Plotnichenko, V. O. Sokolov, E. B. Kryukova, and E. M. Dianov, J. Non-Cryst. Solids **270,** 20 (2000).
15. M. Wachtler, A. Speghini, S. Pigorini, R. Rolli, and M. Bettinelli, J. Non-Cryst. Solids **217,** 111 (1997).
16. M. Nogami and Y. Abe, J. Non-Cryst. Solids **197,** 73 (1996).
17. R. C. Faria and L.-O. S. Bulhões, J. Electrochem. Soc. **141,** L29 (1994).
18. A. Lu, Y. Xie, X. Zhang, and R. Lu, J. Chin. Ceram. Soc. (in Chinese) **23,** 106 (1995).
19. H.-P. Xia, H.-W. Song, J.-W. Wang, J.-L. Zhang, J.-H. Wang, J.-H. Zhang, Q.-H. Nie, and T.-F. Xu, Chin. Phys. Lett. **20,** 571 (2003).